

Federated Virtual Learning on Heterogeneous Data with Local-global Distillation

Chun-Yin Huang¹ Ruinan Jin¹ Can Zhao² Daguang Xu² Xiaoxiao Li¹

Abstract

Despite Federated Learning (FL)’s trend for learning machine learning models in a distributed manner, it is susceptible to performance drops when training on heterogeneous data. Recently, dataset distillation has been explored in order to improve the efficiency and scalability of FL by creating a smaller, synthetic dataset that retains the performance of a model trained on the local private datasets. We discover that using distilled local datasets can amplify the heterogeneity issue in FL. To address this, we propose a new method, called **F**ederated **V**irtual Learning on **H**eterogeneous Data with **L**ocal-**G**lobal **D**istillation (FEDLGD), which trains FL using a smaller synthetic dataset (referred as *virtual data*) created through a combination of local and global distillation. Specifically, to handle synchronization and class imbalance, we propose iterative distribution matching to allow clients to have the same amount of balanced *local virtual data*; to harmonize the domain shifts, we use federated gradient matching to distill *global virtual data* that are shared with clients without hindering data privacy to rectify heterogeneous local training via enforcing local-global feature similarity. We experiment on both benchmark and real-world datasets that contain heterogeneous data from different sources. Our method outperforms *state-of-the-art* heterogeneous FL algorithms under the setting with a very limited amount of distilled virtual data.

1. Introduction

Federated Learning (FL) (McMahan et al., 2017) has become a popular solution for different institutions to collaboratively train machine learning models without pooling

*Equal contribution ¹Department of Electrical and Computer Engineering, The University of British Columbia, Vancouver, Canada ²NVIDIA, Santa Clara, USA. Correspondence to: Xiaoxiao Li <xiaoxiao.li@ece.ubc.ca>.

Preliminary work.

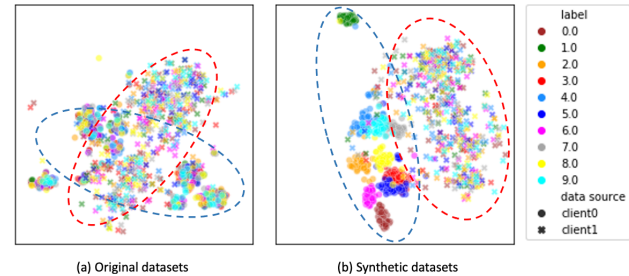


Figure 1. Distilled local datasets can worsen heterogeneity in FL. tSNE plots of (a) original datasets and (b) distilled virtual datasets of USPS (client 0) and SynthDigits (client 1). The two distributions are marked in red and blue. We observe fewer overlapped \circ and \times in (b) compared with (a), indicating higher heterogeneity between two clients after distillation.

private data together. Typically, it involves a central server and multiple local clients; then the model is trained via aggregation of local network parameter updates on the server side iteratively. FL is widely accepted in many areas, such as computer vision, natural language processing, and medical image analysis.

On the one hand, clients with different amounts of data cause asynchronization and affect the efficiency of FL systems. Dataset distillation (Wang et al., 2018; Cazenavette et al., 2022; Zhao et al., 2021; Zhao & Bilen, 2021; 2023) addresses the issue by only summarizing smaller synthetic datasets from the private local datasets to ensure each client owns the same amount of data. We refer this underexplored strategy as *federated virtual learning* as the models are trained from synthetic data (Xiong et al., 2022; Goetz & Tewari, 2020; Hu et al., 2022). These methods have been found to perform better than model-synchronization-based FL approaches while also requiring fewer server-client interactions.

On the other hand, due to different data collection protocols, data from different clients inevitably face heterogeneity problems with domain shift, which means data may not be independent and identically distributed (iid) among clients. Heterogeneous data distribution among clients becomes a key challenge in FL, as aggregating model parameters from non-iid feature distributions suffers from client drift (Karimreddy et al., 2020) and diverges the global model update(Li

et al., 2020b).

We observe that using locally distilled datasets can amplify the heterogeneity issue. Figure 1 shows the tSNE plots of two different datasets, USPS (Netzer et al., 2011) and SynthDigits (Ganin & Lempitsky, 2015), each considered as a client. tSNE takes the original and distilled virtual images as input and embed them into 2D planes. One can observe that the distribution becomes diverse after distillation.

To alleviate the problem of data heterogeneity in classical FL settings, two main orthogonal approaches can be taken. *Approach 1* aims to minimize the difference between the local and global model parameters to improve convergence (Li et al., 2020a; Karimireddy et al., 2020; Wang et al., 2020). *Approach 2* enforces consistency in local embedded features using anchors and regularization loss (Tang et al., 2022; Zhou et al., 2022; Ye et al., 2022). The first approach can be easily applied to distilled local datasets, while the second approach has limitations when adapting to federated virtual learning. Specifically, VHL (Tang et al., 2022) sampling global anchors from untrained StyleGAN (Karras et al., 2019) fail to handle amplified heterogeneity after dataset distillation. Other methods, such as those that rely on external global data (Zhou et al., 2022), or feature sharing from clients (Ye et al., 2022), are less practical, as they pose greater data privacy risks compared to classical FL settings¹. Without hindering data privacy, developing strategies following *approach 2* for federated virtual learning on heterogeneous data remains open questions on 1) *how to set up global anchors for locally distilled datasets* and 2) *how to select the proper regularization loss(es)*.

To this end, we propose FEDLGD, a federated virtual learning method with local and global distillation. We propose *iterative distribution matching* in local distillation by comparing the feature distribution of real and synthetic data using an evolving feature extractor. The local distillation results in smaller sets with balanced class distributions, achieving efficiency and synchronization while avoiding class imbalance. FEDLGD updates the local model on local distilled synthetic datasets (named *local virtual data*). We found that training FL with local virtual data can exacerbate heterogeneity in feature space if clients' data has domain shift (Figure. 1). Therefore, unlike previously proposed federated virtual learning methods that rely solely on local distillation (Goetz & Tewari, 2020; Xiong et al., 2022; Hu et al., 2022), we also propose a novel and efficient method, *federated gradient matching*, that integrated well with FL to distill global virtual data as anchors on the server side. This approach aims to alleviate domain shifts among clients by promoting similarity between local and global features. Note that we only share local model parameters

¹Note that FedFA (Zhou et al., 2022), and FedFM (Ye et al., 2022) are unpublished works proposed concurrently with our work

w.r.t. distilled data. Thus, the privacy of local original data is preserved. We conclude our contributions as follows:

- This paper focuses on an important but underexplored FL setting in which local models are trained on small distilled datasets, which we refer to as *federated virtual learning*. We design two effective and efficient dataset distillation methods for FL.
- We are *the first* to reveal that when datasets are distilled from clients' data with domain shift, the heterogeneity problem can be *exacerbated* in the federated virtual learning setting.
- We propose to address the heterogeneity problem by mapping clients to similar features regularized by gradually updated global virtual data using averaged client gradients.
- Through comprehensive experiments on benchmark and real-world datasets, we show that FEDLGD outperforms existing state-of-the-art FL algorithms.

2. Related Work

2.1. Dataset Distillation

Data distillation aims to improve data efficiency by distilling the most essential feature in a large-scale dataset (e.g., datasets comprising billions of data points) into a certain terse and high-fidelity dataset. For example, Gradient Matching (Zhao et al., 2021) is proposed to make the deep neural network produce similar gradients for both the terse synthetic images and the original large-scale dataset. Besides, (Cazenavette et al., 2022) propose matching the model training trajectory between real and synthetic data to guide the update for distillation. Another popular way of conducting data distillation is through Distribution Matching (Zhao & Bilen, 2023). This strategy instead, attempts to match the distribution of the smaller synthetic dataset with the original large-scale dataset. It brings in significantly improved the distillation efficiency. Moreover, recent studies have justified that data distillation also preserves privacy (Dong et al., 2022; Carlini et al., 2022b), which is critical in federated learning. Other modern data distillation strategies can be found here (Sachdeva & McAuley, 2023).

2.2. Heterogeneous Federated Learning

FL performance downgrading on non-iid data is a critical challenge. A variety of FL algorithms have been proposed ranging from global aggregation to local optimization to handle this heterogeneous issue. *Global aggregation* improves the global model exchange process for better unitizing the updated client models to create a powerful server model. FedNova (Wang et al., 2020) notices an imbalance among

different local models caused by different levels of training stage (e.g., certain clients train more epochs than others) and tackles such imbalance by normalizing and scaling the local updates accordingly. Meanwhile, FedAvgM (Hsu et al., 2019) applies the momentum to server model aggregation to stabilize the optimization. Furthermore, there are strategies to refine the server model from learning client models such as FedDF (Lin et al., 2020) and FedFTG (Zhang et al., 2022). *Local training optimization* aims to explore the local objective to tackle the non-iid issue in FL system. FedProx (Li et al., 2020a) straightly adds L_2 norm to regularize the client model and previous server model. Scaffold (Karimireddy et al., 2020) adds the variance reduction term to mitigate the “clients-drift”. Also, MOON (Li et al., 2021b) brings mode-level contrastive learning to maximize the similarity between model representations to stable the local training. There is another line of works (Ye et al., 2022; Tang et al., 2022) proposed to use a global *anchor* to regularize local training. Global anchor can be either a set of virtual global data or global virtual representations in feature space. However, in (Tang et al., 2022), the empirical global anchor selection may not be suitable for data from every distribution as they don’t update the anchor according to the training datasets.

2.3. Datasets Distillation for FL

Dataset distillation for FL is an important topic but was just attracted attention in the field. It trains model on distilled synthetic datasets, thus we refer it as federated virtual learning. It can help with FL synchronization and improve training efficiency by condensing every client’s data into a small set. To the best of our knowledge, there are few published works on distillation in FL. Concurrently with our work, some studies (Goetz & Tewari, 2020; Xiong et al., 2022; Hu et al., 2022) distill datasets locally and share the distilled datasets with other clients/servers. Although privacy is protected against *currently* existing attack models, we consider sharing local distilled data a dangerous move. Furthermore, none of the existing work has addressed the heterogeneity issue.

3. Method

In this section, we will describe the problem setup, introduce the key technical contributions and rational of the design for FEDLGD, and explain the overall training pipeline.

3.1. Setup for Federated Virtual Learning

We start with describing the classical FL setting. Suppose there are N parties (clients) who own local datasets (D_1, \dots, D_N) , and the goal of a classical FL system, such as FedAvg (McMahan et al., 2017), is to train a global model with parameters θ on the distributed datasets ($D \equiv$

$\bigcup_{i \in [N]} D_i$). The objective function is written as:

$$\mathcal{L}(\theta) = \sum_{i=1}^N \frac{|D_i|}{|D|} \mathcal{L}_i(\theta), \tag{1}$$

where $\mathcal{L}_i(w)$ is the empirical loss of client i .

In practice, different clients in FL may have variant amounts of training samples, leading to asynchronized updates. In this work, we focus on a new type of FL training method – federated virtual learning, that trains on distilled datasets for efficiency and synchronization (discussed in Sec.2.3.) Federated virtual learning synthesizes local virtual data \tilde{D}_i for client i for $i \in [N]$ and form $\tilde{D} \equiv \bigcup_{i \in [N]} \tilde{D}_i$. Typically, $|\tilde{D}_i| \ll |D_i|$ and $|\tilde{D}_i| = |\tilde{D}_j|$. A basic setup for federated virtual learning is to replace D_i with \tilde{D}_i in Eq (1), namely FL model is trained on the virtual datasets rather than the original local private datasets. Following the setting in FedDM (Xiong et al., 2022), the client cannot share gradients w.r.t. the original data for privacy concern.

3.2. Overall Pipeline

The overall pipeline of our proposed method contains three stages, including 1) *initialization*, 2) *iterative local-global distillation*, and 3) *federated virtual learning*.

We begin with the initialization of the server on global virtual data \tilde{D}^g and network parameters θ_0^g ; both are shared with clients. Clients initialize local model weights θ_0^c and prepare initial local virtual data \tilde{D}^c by performing one round of distribution matching (DM) (Zhao & Bilen, 2023).

Then, we will warm up federated virtual learning by preparing our local and global virtual data using our proposed *local-global* distillation strategies in Sec. 3.3.1 and 3.3.2. This step is performed for a few (τ) iterations to update f_θ using $\mathcal{L}_{\text{total}}$ (Eq 3), \tilde{D}^g using $\mathcal{L}_{\text{Dist}}$ (Eq 5), and \tilde{D}^c using \mathcal{L}_{MMD} (Eq 2). In this stage, we generate the same amount of class-balanced virtual data for each client and server.

Finally, after obtaining local and global virtual data \tilde{D}^g and \tilde{D}^c at $t = \tau$, we use \tilde{D}^g as regularization anchor to calculate \mathcal{L}_{Con} (Eq. 4). We perform ordinary FedAvg (McMahan et al., 2017) on local virtual data \tilde{D}^c to further continue federated virtual learning in stage 3 using $\mathcal{L}_{\text{total}}$ (Eq 3). We depict the overview of FEDLGD pipeline in Figure 2. We provide implementation details and the anonymous link to our code in the Appendix.

3.3. FL with Local-Global Dataset Distillation

3.3.1. LOCAL DATA DISTILLATION

Our purpose is to decrease the number of local data to achieve efficient training to meet the following goals. First of all, we hope to synthesize virtual data conditional on class

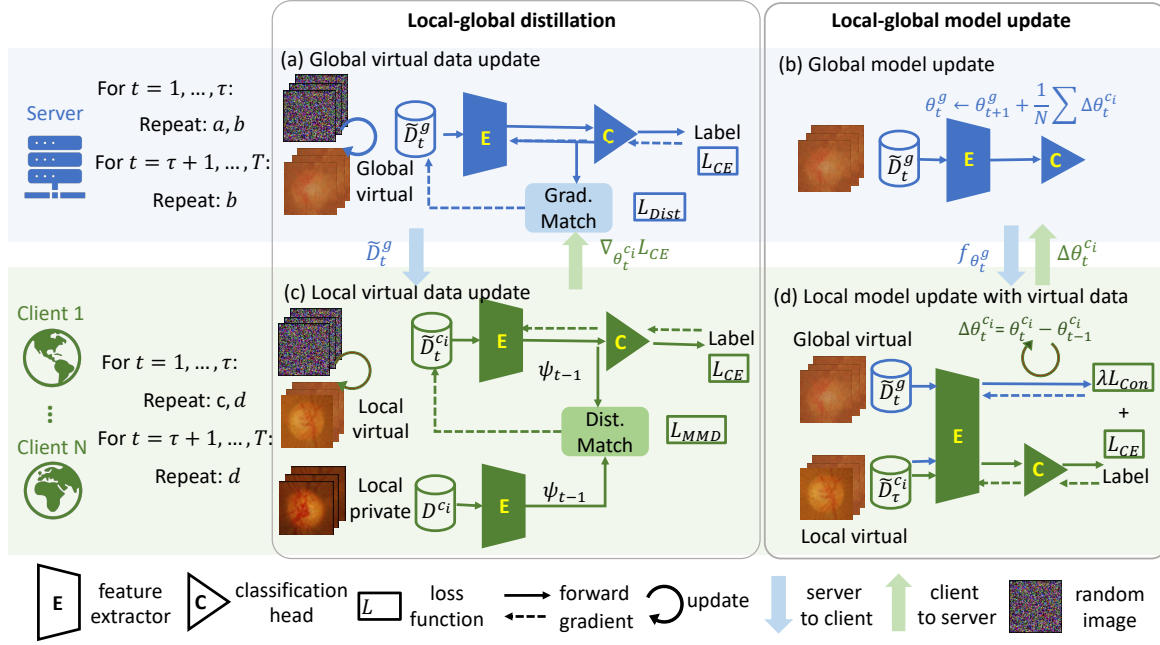


Figure 2. Overview pipeline for FEDLGD. Step 1 ($t = 0$): initialize models, global virtual data, and the local virtual data by DM (Zhao & Bilen, 2023) for each client (skipped in the figure to make the following procedures more clear). Step 2 ($t = 1$ to τ): server uses aggregated gradients from cross-entropy loss to update global virtual data (a) and update the global model (b). Step 3 ($t = 1$ to τ): clients will not only update local models (d) but also refine the local virtual data with the latest network parameters (c). We repeat Step 2 and 3 iteratively for τ epochs. We term this procedure as Iterative Local-global Distillation. Step 4 ($t = \tau$ to T): we continue to perform (Local-global model updates but stop updating virtual data. The FL training is simplified to an ordinary FL pipeline on local virtual data (federated virtual learning), but clients will continue to use global virtual data to regularize local training.

labels to achieve class-balanced virtual datasets. Second, we hope to distill local data that is the best suit for the classification task. Last but not least, the process should be efficient due to the limited computational resource locally. To this end, we design Iterative Distribution Matching to fulfill our purpose.

Iterative distribution matching. To achieve better local virtual datasets, we proposed a novel distillation strategy, named iterative distribution matching, which is a distribution-based technique that gradually improves distillation quality during FL training. To begin with, we split a model into two parts, feature extractor ψ (shown as E in figure 2) and classification head h (shown as C in figure 2). The whole classification model is defined as $f_\theta = h_\beta \circ \psi_w$. Feature extractor embeds input data from the original space to a lower dimensional space, while the classification head projects the embedding to the corresponding labels. The high-level idea of distribution matching can be described as follows. Given a feature extractor $\psi_w : \mathbb{R}^d \rightarrow \mathbb{R}^{d'}$, we want to generate \tilde{D} so that $\psi_w(x) \approx \psi_w(x')$ where $x \in D$ and $x' \in \tilde{D}$. To optimize w , we use maximum mean discrepancy (MMD) (Gretton et al., 2012) to estimate the distance between D and \tilde{D} . To distill local data during FL efficiently that best fits our task, we intend to use the up-to-

date server model’s feature extractor as our kernel function to distill better virtual data. Since we can’t obtain ground truth distribution of local data, we utilize empirical MMD as our loss function for local virtual distillation:

$$\mathcal{L}_{MMD} = \sum_k^K \left\| \frac{1}{|D_k^c|} \sum_{i=1}^{|D_k^c|} \psi_w^t(x_i) - \frac{1}{|\tilde{D}_k^{c,t}|} \sum_{j=1}^{|\tilde{D}_k^{c,t}|} \psi_w^t(\tilde{x}_j^t) \right\|^2, \quad (2)$$

where ψ_w^t and $\tilde{D}^{c,t}$ are the server feature extractor and local virtual data from the latest global iteration t . Following (Zhao et al., 2021; Zhao & Bilen, 2023), we apply the differentiable Siamese virtual data \tilde{D}^c . K is the total number of classes, and we sum over MMD loss calculated per class $k \in [K]$. In such a way, we can generate balanced local virtual data by optimizing the same number of virtual data per class.

Although such an efficient distillation strategy is inspired by DM (Zhao & Bilen, 2023), we highlight the following two key differences between our iterative distribution matching with theirs. First, DM uses randomly initialized deep neural networks to extract features, whereas we use trained FL models with task-specific supervised loss. We believe *iterative updating* on the clients’ data using the up-to-date network parameters can generate better task-specific

local virtual data. Our intuition comes from the recent success of the empirical neural tangent kernel for data distribution learning and matching (Mohamadi & Sutherland, 2022; Franceschi et al., 2022). Second, the feature extractors in FEDLGD are iteratively updated during training. We apply DM (Zhao & Bilen, 2023) to the baseline FL methods and demonstrate the effectiveness of our proposed iterative strategy in Sec. 4. Furthermore, note that FEDLGD only requires a few hundreds of local distillations steps using the local model’s feature distribution, which is more computationally efficient than other bi-level dataset distillation methods (Zhao et al., 2021; Cazenavette et al., 2022).

Heterogeneity in using locally distilled datasets. Data collected in different sites may have different distributions due to different collecting protocols and populations. Such heterogeneity will degrade the performance of FL. Worse yet, we found increased data heterogeneity among clients when federatively training with distilled local virtual data (see Figure 1). We aim to alleviate the dataset shift by adding a regularization term in feature space to our total loss function for local model updating, which is inspired by (Tang et al., 2022; Khosla et al., 2020):

$$\mathcal{L}_{\text{total}} = \mathcal{L}_{\text{CE}}(\tilde{D}^g, \tilde{D}^c; w) + \lambda \mathcal{L}_{\text{Con}}(\tilde{D}^g, \tilde{D}^c), \quad (3)$$

and

$$\mathcal{L}_{\text{Con}} = \sum_{i \in I} \frac{-1}{|P(i)|} \sum_{p \in P(i)} \log \frac{\exp(z_i \cdot z_p / \tau_{\text{temp}})}{\sum_{a \in A(i)} \exp(z_i \cdot z_a / \tau_{\text{temp}})}, \quad (4)$$

where \mathcal{L}_{CE} is the cross-entropy measured on the virtual data and its corresponding and \mathcal{L}_{Con} is the supervised contrastive loss where I is the collection of all indices, $A(i)$ indicates all the local and global virtual data indices without i ($A(i) \equiv I \setminus \{i\}$), $z = \psi(x)$ is the output of feature extractor, $P(i)$ represents the set of images belonging to the same class y_i without data i , and τ_{temp} is a scalar temperature parameter. In such a way, global virtual data can be served for calibration, e.,g., z_i is from \tilde{D}^g as an anchor and z_p is from \tilde{D}^c . At this point, a critical problem arises: *How do we generate global virtual data?*

3.3.2. GLOBAL DATA DISTILLATION

To address the aforementioned question, we provide an affirmative solution by generating global data. Although distribution-based matching is efficient, local clients may not share their features due to privacy concerns. Therefore, we propose to leverage local clients’ averaged gradients to distill global virtual data. In addition, the distilled global virtual data could be used in Eq. (4). We term our global data distillation method as *Federated Gradient Matching*.

Federated gradient matching. The concept of gradient-based dataset distillation is to minimize the distance between gradients from model parameters trained by original

data and distilled data. It is usually considered as a learning-to-learn problem because the procedure consists of model updates and distilled data updates. Zhao *et al.* (Zhao et al., 2021) studies gradient matching in the centralized setting via bi-level optimization that iteratively optimizes the virtual data, which is further used to optimize the model to obtain similar utility as training on the original datasets. However, the implementation proposed by Zhao *et al.* is not appropriate for our specific context because there are two fundamental differences in our setting: 1) for model updating, the gradient-distilled dataset is on the server and will not directly optimize the targeted task; 2) for virtual data update, the ‘optimal’ model comes from optimized local model aggregation. These two steps can naturally be embedded in local model updating and global virtual data distillation from averaged local gradients in FL. Furthermore, when clients update locally, the server will use the aggregated local gradients in the previous round to distill global data.

First, we define a distance loss $\mathcal{L}_{\text{Dist}}$ for gradient matching:

$$\mathcal{L}_{\text{Dist}} = \text{Dist}(\nabla_{\theta} \mathcal{L}_{\text{CE}}^{\tilde{D}^g}(\theta), \nabla_{\theta} \mathcal{L}_{\text{CE}}^{\tilde{D}^c}(\theta)) \quad (5)$$

where \tilde{D}^c and \tilde{D}^g denote local and global virtual data, $\nabla_{\theta} \mathcal{L}_{\text{CE}}^{\tilde{D}^c}$ is the average client gradient. Our proposed federated gradient matching optimize as follows:

$$\min_{\tilde{D}^g} \mathcal{L}_{\text{Dist}}(\theta) \quad \text{subject to} \quad \theta = \frac{1}{N} \theta^{c_i^*},$$

where $\theta^{c_i^*} = \arg \min_{\theta} \mathcal{L}_i(\tilde{D}^c)$ is the optimal local model weights of client i at a certain round t .

Furthermore, noting that compared with FedAvg (McMahan et al., 2017), there is no additional client information shared for global distillation. We also note the approach seems similar to the gradient inversion attack (Zhu et al., 2019) but we consider averaged gradients w.r.t. local virtual data, and the method potentially defends inference attack better (Appendix Figure 13), which is also implied by (Xiong et al., 2022; Dong et al., 2022). Privacy preservation can be further improved by employing differential privacy (Abadi et al., 2016) in gradient sharing, but this is not the main focus of our work.

3.3.3. PROPER INITIALIZATION FOR DISTILLATION

In the original papers (Zhao et al., 2021; Zhao & Bilen, 2023), there are two initialization strategies for distilling virtual dataset: sampling and Gaussian noise. For sampling initialization, a given number of images are randomly selected for every class in the dataset initialization. This method has been shown to reach the best distillation performance but brings privacy hazard in our FL setting, since part of the real images are exposed to other FL participants,

which may be under the risk of various data exposition attacks, such as the gradient inversion attack (Huang et al., 2021). On the other hand, distilled images can be initialized from normal Gaussian noise ($x \sim \mathcal{N}(0, 1)$). However, such a strategy creates difficulties for the convergence of the model and, moreover, yields low-fidelity distillation data. In this study, we propose to initialize the distilled data using statistics from the data set per class to take care of both privacy concerns and model performance. Specifically, each client calculates the statistics of its own data for each class, denoted as μ_i^c, σ_i^c , and then initializes the distillation images per class, $x \sim \mathcal{N}(\mu_i^c, \sigma_i^c)$, where c and i represent each client and categorical label. The server asks each client to share the statistics, aggregates the information $\mu_i^g = \sum_{c \in C} \frac{1}{c} \mu_i^c$ and $\sigma_i^g = \sum_{c \in C} \frac{1}{c} \sigma_i^c$, and initializes their virtual images as $x \sim \mathcal{N}(\mu_i^g, \sigma_i^g)$. In this way, no real data is shared with any participant in the FL system.

4. Experiment

To evaluate FEDLGD, we consider the FL setting in which clients contain data from different domains while performing the same task. Specifically, we compare with multiple baselines on benchmark datasets DIGITS (Sec. 4.2) and RETINA (Sec. 4.3). Additionally, we perform comprehensive ablation studies on different hyperparameters, and alternative loss choices, and demonstrate FEDLGD’s effectiveness for mitigating heterogeneity. More results are available in Appendix B.

4.1. Training and Evaluation Setup

Model architecture. We conduct the ablation study to explore the effect of different deep neural networks’ performance under FEDLGD. Specifically, we adapt ResNet18 (He et al., 2016) and ConvNet in our study. To achieve the best performance, we apply the same architecture to perform both the local distillation task and the classification task, as this combination is justified to have the best output (Zhao et al., 2021; Zhao & Bilen, 2023). The model details are presented in Appendix B.4.

Comparison methods. We compare the classification models trained using state-of-the-art (SOTA) FL algorithms, FedAvg (McMahan et al., 2017), FedProx (Li et al., 2020b), FedNova (Wang et al., 2020), Scaffold (Karimireddy et al., 2020), MOON (Li et al., 2021b), and VHL (Tang et al., 2022)². We directly use local virtual data from our initialization stage with DM for FL methods other than ours. VHL (Tang et al., 2022) generates global virtual data using untrained StyleGAN (Karras et al., 2019), and the global virtual data are not updated during training. A detailed

²The detailed information of the methods can be found in Appendix C.

illustration of the alternative methods is explained in Appendix C. We will report the accuracy of each client’s testing set and the unweighted average accuracy among clients.

FL training setup. For model training, we use the SGD optimizer with a learning rate of 10^{-2} for DIGITS and 10^{-3} for RETINA. If not specified, our default setting for local update epochs is $E = 1$, the default setting for total update rounds is 100, and the batch size is 32. The default local distillation step using iterative distribution matching is 200. The default federated global matching step is 2000. The experiments are run on NVIDIA GeForce RTX 3090 Graphics cards with PyTorch.

4.2. Benchmark Experiment

Datasets. We use the following datasets for our benchmark experiments: DIGITS = {MNIST (LeCun et al., 1998), SVHN (Netzer et al., 2011), USPS (Hull, 1994), SynthDigits (Ganin & Lempitsky, 2015), MNIST-M (Ganin & Lempitsky, 2015)}. Each dataset in DIGITS contains handwritten, real street and synthetic digit images of 0, 1, \dots , 9. As a result, we have five clients in benchmark experiments, and image size is 28×28 .

Comparison with baselines under different settings. To validate the effectiveness of FEDLGD, we first compare it with the alternative FL methods varying on two important factors: Image-per-class (IPC) and different deep neural network architectures. We use $IPC \in \{10, 50\}$ and $arch \in \{\text{ResNet18(R)}, \text{ConvNet(C)}\}$ to examine the performance of SOTA models and FEDLGD using distilled DIGITS. Note that we use same IPC for global virtual data and each local virtual data. Table 1 shows the test accuracies of DIGITS experiments. In addition to testing with original test sets, we also show the unweighted averaged test accuracy different re(Average). One can observe that for each FL algorithm, ConvNet(C) always has the best performance regardless of the selection of IPC. The observation is consistent with (Zhao & Bilen, 2023). It is also shown that using IPC=50 always outperforms IPC=10 as our expectation since more data are available for training. Overall, FEDLGD outperforms other SOTA methods, where on average accuracy, FEDLGD increases the best test accuracy results among the baseline methods of 1.7% (IPC=10, arch=C), 8.9% (IPC=10, arch=R), 3.4% (IPC=50, arch=C) and 4.1% (IPC=50, arch=R). VHL (Tang et al., 2022) is the closest strategy to FEDLGD and achieves the best performance among the baseline methods, indicating that the feature alignment solutions are promising for handling heterogeneity in federated virtual learning. However, VHL is still worse than FEDLGD, and underperformance may result from the difference in synthesizing global virtual data. VHL (Tang et al., 2022) uses untrained StyleGAN (Karras et al., 2019) to generate global virtual data without further updating. On

Table 1. Test accuracy for DIGITS under different images per class (IPC) and model architectures. R and C stand for ResNet18 and ConvNet, respectively. IPC indicates the image per class, and we have IPC = 10 and 50. We have five clients (MNIST, SVHN, USPS, SynthDigits, and MNIST-M) containing data from different domains. ‘Average’ is the unweighted average of all the clients. The best performance under different models is emphasized as **bold**. The best results on ConvNet are marked in **red** and in bold black for ResNet18.

DIGITS		MNIST		SVHN		USPS		SynthDigits		MNIST-M		Average	
IPC		10	50	10	50	10	50	10	50	10	50	10	50
FedAvg	R	73.0	92.5	20.5	48.9	83.0	89.7	13.6	28.0	37.8	72.3	45.6	66.3
	C	94.0	96.1	65.9	71.7	91.0	92.9	55.5	69.1	73.2	83.3	75.9	82.6
FedProx	R	72.6	92.5	19.7	48.4	81.5	90.1	13.2	27.9	37.3	67.9	44.8	65.3
	C	93.9	96.1	66.0	71.5	90.9	92.9	55.4	69.0	73.7	83.3	76.0	82.5
FedNova	R	75.5	92.3	17.3	50.6	80.3	90.1	11.4	30.5	38.3	67.9	44.6	66.3
	C	94.2	96.2	65.5	73.1	90.6	93.0	56.2	69.1	74.6	83.7	76.2	83.0
Scaffold	R	75.8	93.4	16.4	53.8	79.3	91.3	11.2	34.2	38.3	70.8	44.2	68.7
	C	94.1	96.3	64.9	73.3	90.6	93.4	56.0	70.1	74.6	84.7	76.0	83.6
MOON	R	15.5	80.4	15.9	14.2	25.0	82.4	10.0	11.5	11.0	35.4	15.5	44.8
	C	85.0	95.5	49.2	70.5	83.4	92.0	31.5	67.2	56.9	82.3	61.2	81.5
VHL	R	87.8	94.8	29.7	57.6	87.5	92.6	17.9	41.5	55.0	75.1	55.6	72.3
	C	95.0	96.8	68.4	72.8	92.0	94.9	60.8	70.0	76.6	80.0	80.2	82.7
FEDLGD	R	92.4	95.3	46.2	63.3	87.1	91.6	27.2	51.3	69.9	80.4	64.5	76.4
	C	96.3	97.4	69.9	76.1	92.8	95.5	64.6	77.5	85.7	88.5	81.9	87.0

Table 2. Varying batch size in FEDLGD on DIGITS. M, S, U, Syn, MM, and Avg stand for MNIST, SVHN, USPS, SynthDigits, MNIST-M, Averaged, respectively.

DIGITS	M	S	U	Syn	MM	Avg
8	97.2	76.3	95.4	73.8	86.1	85.8
16	97.0	77.0	94.9	75.3	84.7	85.8
32	97.4	76.1	95.5	77.5	88.5	87.0
64	97.5	76.8	94.8	77.8	89.0	87.2

the contrary, we update our global virtual data during FL training.

Effect of regularization loss FEDLGD uses supervised contrastive loss \mathcal{L}_{Con} as a regularization term to encourage local and global virtual data embedding into a similar feature space. To demonstrate the effectiveness of the regularization term in FEDLGD, we first perform ablation studies to replace \mathcal{L}_{Con} with an alternative distribution similarity measurement, MMD loss, with different coefficients λ ranging from 0.1 to 20. Table 3 shows the average test accuracy. Using supervised contrastive loss gives us better and more stable performance with different coefficient choices.

Furthermore, to explain the effect of the proposed regularization loss on feature representation, we embed the latent feature before fully-connected layers to a 2D space using tSNE (Van der Maaten & Hinton, 2008) in Figure 3. For the model trained with FedAvg (Figure 3(a)), features from two clients (\times and \circ) are closer to their own distribution regardless of the labels(color). In Figure 3(b), we perform local training, including local virtual data and global virtual data but without regularization term (Eq. 4). Figure 3(c) shows FEDLGD with regularization, data from different clients with the same label are grouped together. This indicates that our regularization with global virtual data is useful for learning homogeneous feature representations.

Table 3. Different regularization loss under different coefficients.

Loss	MMD				Contrastive			
Coeff	0.1	1	10	20	0.1	1	10	20
DIGITS	85.2	81.0	23.6	15.3	86.0	83.9	87.0	87.2

Table 4. Test accuracy for different combinations on (local, global) distillation iterations with FEDLGD.

(100, 500)	(100, 1000)	(100, 2000)	(200, 500)	(200, 1000)	(200, 2000)	(500, 500)	(500, 1000)	(500, 2000)
86.6	86.7	87.2	87.0	86.3	87.0	86.8	86.1	87.1

Analysis of batch size Batch size is another key factor for training the model and our distilled data. We vary the batch size $\in \{8, 16, 32, 64\}$ to train models for DIGITS with the fixed default learning rate. We show the effect of batch size in Table 2 reported on average testing accuracy. One can observe that the performance is slightly better with moderately large batch size might for three reasons: 1) involve a larger number of data in one update and thus makes the model update direction more stable; 2) decrease local update iterations per round, causing gradients to decrease to zero more slowly with the fixed learning rate, which can benefit federated global data distillation; and 3) Similar with the observation in (Khosla et al., 2020) and (Tang et al., 2022), contrastive learning pulls data of the same class together in \mathcal{L}_{Con} and large batch size can benefit its convergence. However, larger batch size requires more powerful computation resources for clients. Overall, the results are generally stable with different batch size choices.

Analysis of distillation iterations Table 4 shows the average test accuracy for different combinations on (local, global) distillation iterations with FEDLGD. The local distillation rounds range from 100, 200 to 500 and the global distillation rounds range from 500, 1000, to 2000. As can be seen, FEDLGD not only yields stable test accuracy in

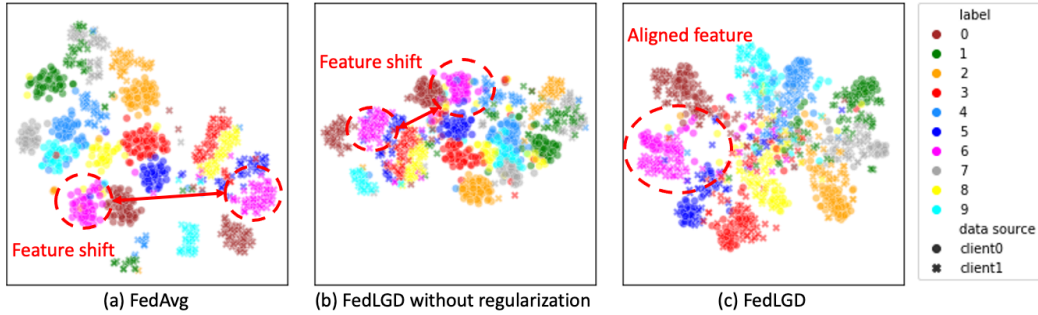


Figure 3. tSNE plots on feature space for FedAvg, FEDLGD without regularization, and FEDLGD. One can observe regularizing training with our global virtual data can rectify feature shift among different clients.

Table 5. Test accuracy for RETINA experiments under different model architectures and IPC=10. R and C stand for ResNet18 and ConvNet, respectively. We have 4 clients: Drishti(D), Acrima(A), Rim(Ri), and Refuge(Re), respectively. We also show the averaged test accuracy (Average). The best results on ConvNet are marked in red and in bold for ResNet18. The same accuracy for different methods is due to the limited number of testing samples.

RETINA		D	A	Ri	Re	Avg
FedAvg	R	31.6	71.0	52.0	78.5	58.3
	C	69.4	84.0	88.0	86.5	82.0
FedProx	R	31.6	70.0	52.0	78.5	58.0
	C	68.4	84.0	88.0	86.5	81.7
FedNova	R	31.6	71.0	52.0	78.5	58.3
	C	68.4	84.0	88.0	86.5	81.7
Scaffold	R	31.6	73.0	49.0	78.5	58.0
	C	68.4	84.0	88.0	86.5	81.7
MOON	R	42.1	71.0	57.0	70.0	60.0
	C	57.9	72.0	76.0	85.0	72.7
VHL	R	47.4	62.0	50.0	76.5	59.0
	C	68.4	78.0	81.0	87.0	78.6
FEDLGD	R	57.9	75.0	59.0	77.0	67.2
	C	73.7	82.0	89.0	91.5	84.1

different combinations of the local and global distillation epochs, but also beats all other methods in Table 1.

4.3. Experiment Results on Real-world Dataset

Dataset. For medical dataset, we use the retina image datasets, RETINA = {Drishti (Sivaswamy et al., 2014), Acrima(Diaz-Pinto et al., 2019), Rim (Batista et al., 2020), Refuge (Orlando et al., 2020)}, where each dataset contains retina images from different stations with image size 96×96 , thus forming four clients in FL. We perform binary classification to identify *Glaucomatous* and *Normal*. Example images and distributions can be found in Appendix B.3. Each client has a held-out testing set. In the following experiments, we will use the distilled local virtual training sets for training and test the models on the original testing sets. The sample population statistics for both experiments are available in Table 9 and Table 10 in Appendix B.5.

Comparison with baselines. The results for RETINA ex-

periments are shown in Table 5, where D, A, Ri, Re represent Drishti, Acrima, Rim, and Refuge datasets. We only set IPC=10 for this experiment as clients in RETINA contain much fewer data points. The same as in the previous experiment, we vary $\text{arch} \in \{\text{ConvNet}, \text{ResNet18}\}$. Similarly, ConvNet shows the best performance among architectures, and FEDLGD has the best performance compared to the other methods w.r.t the unweighted averaged accuracy (Avg) among clients. To be precise, FEDLGD increases unweighted averaged test accuracy for 2.1%(versus the best baseline) on ConvNet and 7.2%(versus the best baseline) on ResNet18, respectively. The same accuracy for different methods is due to the limited number of testing samples. We conjecture the reason why VHL (Tang et al., 2022) has lower performance improvement in RETINA experiments is that this dataset is in higher dimensional and clinical diagnosis evidence on fine-grained details, e.g., cup-to-disc ratio and disc rim integrity (Schuster et al., 2020). Therefore, it is difficult for untrained StyleGAN (Karras et al., 2019) to distill larger images. As a result, FEDLGD fails to generate better quality global virtual data for RETINA.

5. Conclusion

In this paper, we introduce a new approach for FL, called FEDLGD. It utilizes iterative distribution matching and federated gradient matching to distill virtual data on both client and server sides, then trains FL models with the distilled datasets. We are the first to reveal that FL on local virtual data can increase heterogeneity. Furthermore, we propose global virtual regularization to effectively harmonize domain shift. Our experiments on benchmark and real medical datasets show that FEDLGD outperforms current state-of-the-art methods in heterogeneous settings. Furthermore, FEDLGD can be combined with other heterogeneous FL methods such as FedProx (Li et al., 2020b) and Scaffold (Karimireddy et al., 2020) to further improve its performance. We believe that this work sheds light on how to effectively mitigate data heterogeneity from dataset distillation perspective and will inspire future work to enhance FL performance, privacy, and efficiency.

References

- Abadi, M., Chu, A., Goodfellow, I., McMahan, H. B., Mironov, I., Talwar, K., and Zhang, L. Deep learning with differential privacy. In *Proceedings of the 2016 ACM SIGSAC conference on computer and communications security*, pp. 308–318, 2016.
- Batista, F. J. F., Diaz-Aleman, T., Sigut, J., Alayon, S., Arnay, R., and Angel-Pereira, D. Rim-one dl: A unified retinal image database for assessing glaucoma using deep learning. *Image Analysis & Stereology*, 39(3):161–167, 2020.
- Carlini, N., Chien, S., Nasr, M., Song, S., Terzis, A., and Tramer, F. Membership inference attacks from first principles. In *2022 IEEE Symposium on Security and Privacy (SP)*, pp. 1897–1914. IEEE, 2022a.
- Carlini, N., Feldman, V., and Nasr, M. No free lunch in” privacy for free: How does dataset condensation help privacy?”. *arXiv preprint arXiv:2209.14987*, 2022b.
- Cazenavette, G., Wang, T., Torralba, A., Efros, A. A., and Zhu, J.-Y. Dataset distillation by matching training trajectories. In *Proceedings of the IEEE/CVF Conference on Computer Vision and Pattern Recognition*, pp. 4750–4759, 2022.
- Diaz-Pinto, A., Morales, S., Naranjo, V., Köhler, T., Mossi, J. M., and Navea, A. Cnns for automatic glaucoma assessment using fundus images: an extensive validation. *Biomedical engineering online*, 18(1):1–19, 2019.
- Dong, T., Zhao, B., and Lyu, L. Privacy for free: How does dataset condensation help privacy? *arXiv preprint arXiv:2206.00240*, 2022.
- Franceschi, J.-Y., De Bézenac, E., Ayed, I., Chen, M., Lamprier, S., and Gallinari, P. A neural tangent kernel perspective of gans. In *International Conference on Machine Learning*, pp. 6660–6704. PMLR, 2022.
- Ganin, Y. and Lempitsky, V. Unsupervised domain adaptation by backpropagation. In *International conference on machine learning*, pp. 1180–1189. PMLR, 2015.
- Goetz, J. and Tewari, A. Federated learning via synthetic data. *arXiv preprint arXiv:2008.04489*, 2020.
- Gretton, A., Borgwardt, K. M., Rasch, M. J., Schölkopf, B., and Smola, A. A kernel two-sample test. *The Journal of Machine Learning Research*, 13(1):723–773, 2012.
- He, K., Zhang, X., Ren, S., and Sun, J. Deep residual learning for image recognition. In *Proceedings of the IEEE conference on computer vision and pattern recognition*, pp. 770–778, 2016.
- Hsu, T.-M. H., Qi, H., and Brown, M. Measuring the effects of non-identical data distribution for federated visual classification. *arXiv preprint arXiv:1909.06335*, 2019.
- Hu, S., Goetz, J., Malik, K., Zhan, H., Liu, Z., and Liu, Y. FedSynth: Gradient compression via synthetic data in federated learning. *arXiv preprint arXiv:2204.01273*, 2022.
- Huang, Y., Gupta, S., Song, Z., Li, K., and Arora, S. Evaluating gradient inversion attacks and defenses in federated learning. *Advances in Neural Information Processing Systems*, 34:7232–7241, 2021.
- Hull, J. J. A database for handwritten text recognition research. *IEEE Transactions on pattern analysis and machine intelligence*, 16(5):550–554, 1994.
- Karimireddy, S. P., Kale, S., Mohri, M., Reddi, S., Stich, S., and Suresh, A. T. Scaffold: Stochastic controlled averaging for federated learning. In *International Conference on Machine Learning*, pp. 5132–5143. PMLR, 2020.
- Karras, T., Laine, S., and Aila, T. A style-based generator architecture for generative adversarial networks. In *Proceedings of the IEEE/CVF conference on computer vision and pattern recognition*, pp. 4401–4410, 2019.
- Khosla, P., Teterwak, P., Wang, C., Sarna, A., Tian, Y., Isola, P., Maschinot, A., Liu, C., and Krishnan, D. Supervised contrastive learning. *Advances in Neural Information Processing Systems*, 33:18661–18673, 2020.
- LeCun, Y., Bottou, L., Bengio, Y., and Haffner, P. Gradient-based learning applied to document recognition. *Proceedings of the IEEE*, 86(11):2278–2324, 1998.
- Li, Q., Diao, Y., Chen, Q., and He, B. Federated learning on non-iid data silos: An experimental study. *arXiv preprint arXiv:2102.02079*, 2021a.
- Li, Q., He, B., and Song, D. Model-contrastive federated learning. In *Proceedings of the IEEE/CVF Conference on Computer Vision and Pattern Recognition*, pp. 10713–10722, 2021b.
- Li, T., Sahu, A. K., Zaheer, M., Sanjabi, M., Talwalkar, A., and Smith, V. Federated optimization in heterogeneous networks. *Proceedings of Machine Learning and Systems*, 2:429–450, 2020a.
- Li, X., Huang, K., Yang, W., Wang, S., and Zhang, Z. On the convergence of fedavg on non-iid data. *International Conference on Learning Representations*, 2020b.
- Lin, T., Kong, L., Stich, S. U., and Jaggi, M. Ensemble distillation for robust model fusion in federated learning. *Advances in Neural Information Processing Systems*, 33: 2351–2363, 2020.

- McMahan, B., Moore, E., Ramage, D., Hampson, S., and y Arcas, B. A. Communication-efficient learning of deep networks from decentralized data. In *Artificial intelligence and statistics*, pp. 1273–1282. PMLR, 2017.
- Mohamadi, M. A. and Sutherland, D. J. A fast, well-founded approximation to the empirical neural tangent kernel. *arXiv preprint arXiv:2206.12543*, 2022.
- Netzer, Y., Wang, T., Coates, A., Bissacco, A., Wu, B., and Ng, A. Y. Reading digits in natural images with unsupervised feature learning. 2011.
- Orlando, J. I., Fu, H., Breda, J. B., van Keer, K., Bathula, D. R., Diaz-Pinto, A., Fang, R., Heng, P.-A., Kim, J., Lee, J., et al. Refuge challenge: A unified framework for evaluating automated methods for glaucoma assessment from fundus photographs. *Medical image analysis*, 59: 101570, 2020.
- Sachdeva, N. and McAuley, J. Data distillation: A survey. *arXiv preprint arXiv:2301.04272*, 2023.
- Schuster, A. K., Erb, C., Hoffmann, E. M., Dietlein, T., and Pfeiffer, N. The diagnosis and treatment of glaucoma. *Deutsches Ärzteblatt International*, 117(13):225, 2020.
- Shokri, R., Stronati, M., Song, C., and Shmatikov, V. Membership inference attacks against machine learning models. In *2017 IEEE symposium on security and privacy (SP)*, pp. 3–18. IEEE, 2017.
- Sivaswamy, J., Krishnadas, S., Joshi, G. D., Jain, M., and Tabish, A. U. S. Drishti-gs: Retinal image dataset for optic nerve head (onh) segmentation. In *2014 IEEE 11th international symposium on biomedical imaging (ISBI)*, pp. 53–56. IEEE, 2014.
- Tang, Z., Zhang, Y., Shi, S., He, X., Han, B., and Chu, X. Virtual homogeneity learning: Defending against data heterogeneity in federated learning. *arXiv preprint arXiv:2206.02465*, 2022.
- Van der Maaten, L. and Hinton, G. Visualizing data using t-sne. *Journal of machine learning research*, 9(11), 2008.
- Wang, J., Liu, Q., Liang, H., Joshi, G., and Poor, H. V. Tackling the objective inconsistency problem in heterogeneous federated optimization. *Advances in neural information processing systems*, 33:7611–7623, 2020.
- Wang, T., Zhu, J.-Y., Torralba, A., and Efros, A. A. Dataset distillation. *arXiv preprint arXiv:1811.10959*, 2018.
- Xiong, Y., Wang, R., Cheng, M., Yu, F., and Hsieh, C.-J. Feddm: Iterative distribution matching for communication-efficient federated learning. *arXiv preprint arXiv:2207.09653*, 2022.
- Ye, R., Ni, Z., Xu, C., Wang, J., Chen, S., and Eldar, Y. C. Fedfm: Anchor-based feature matching for data heterogeneity in federated learning. *arXiv preprint arXiv:2210.07615*, 2022.
- Zhang, L., Shen, L., Ding, L., Tao, D., and Duan, L.-Y. Fine-tuning global model via data-free knowledge distillation for non-iid federated learning. In *Proceedings of the IEEE/CVF Conference on Computer Vision and Pattern Recognition*, pp. 10174–10183, 2022.
- Zhao, B. and Bilen, H. Dataset condensation with differentiable siamese augmentation. In *International Conference on Machine Learning*, pp. 12674–12685. PMLR, 2021.
- Zhao, B. and Bilen, H. Dataset condensation with distribution matching. In *Proceedings of the IEEE/CVF Winter Conference on Applications of Computer Vision*, pp. 6514–6523, 2023.
- Zhao, B., Mopuri, K. R., and Bilen, H. Dataset condensation with gradient matching. *ICLR*, 1(2):3, 2021.
- Zhou, T., Zhang, J., and Tsang, D. Fedfa: Federated learning with feature anchors to align feature and classifier for heterogeneous data. *arXiv preprint arXiv:2211.09299*, 2022.
- Zhu, H., Xu, J., Liu, S., and Jin, Y. Federated learning on non-iid data: A survey. *Neurocomputing*, 465:371–390, 2021.
- Zhu, L., Liu, Z., and Han, S. Deep leakage from gradients. *Advances in neural information processing systems*, 32, 2019.

Road Map of Appendix Our appendix is organized in five sections. The notation table is in Appendix A, which contains the mathematical notation we used in main paper and appendix. Appendix B lists the details of our experiments, in which Appendix B.1 visualizes the original sample images used in our experiments; Appendix B.2 visualizes the local and global distilled images; Appendix B.3 shows the pixel diagram for the *Digits* and *Retina* datasets for visualizing the heterogeneity of both datasets. Appendix B.4 shows the model architecture that we used in the experiments; Appendix B.5 contains the hyper-parameters that we used to conduct all experiments; Appendix B.6 visualizes our averaged regularization loss for both experiments of both datasets to show our convergence; Appendix B.7 visualizes our server-side synthetic data; Appendix B.8 shows the comparison of different local epochs and the number of global communications in FEDLGD and the state-of-the-art models; Appendix B.9 provides experiments and analysis for the privacy of FEDLGD using membership inference attack. Finally, Appendix C provides a detailed literature review and implementation of the state-of-the-art heterogeneous FL strategies. Our code will be available soon.

A. Notation Table

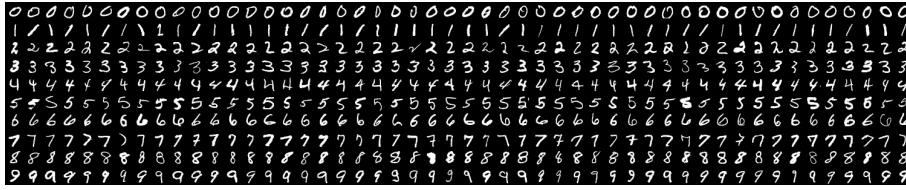
Table 6. Important notations used in the paper.

Notations	Description
d	input dimension
d'	feature dimension
θ	model parameters
ψ	feature extractor
h	projection head
D^g, D^c	original global and local data
\tilde{D}^g, \tilde{D}^c	global and local synthetic data
\tilde{f}^g, \tilde{f}^c	features of global and local synthetic data
$\mathcal{L}_{\text{total}}$	total loss function for virtual federated training
\mathcal{L}_{CE}	cross-entropy loss
$\mathcal{L}_{\text{Dist}}$	Distance loss for gradient matching
\mathcal{L}_{MMD}	MMD loss for distribution matching
\mathcal{L}_{Con}	Contrastive loss for local training regularization
λ	coefficient for local training regularization term
T	total updating iterations
τ	local global distillation iterations

B. Experimental details

B.1. Visualization of the original images

B.1.1. DIGITS DATASET



(a)



(b)



(c)



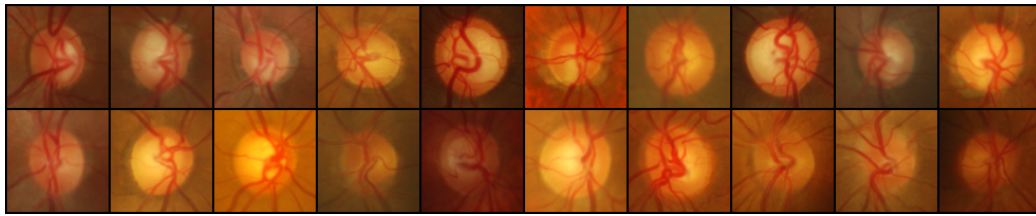
(d)



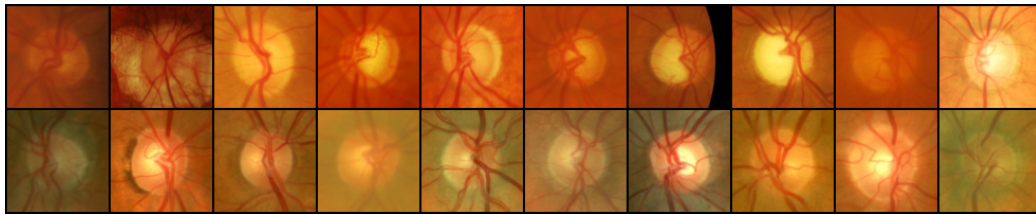
(e)

Figure 4. Visualization of the original digits dataset. (a) visualized the MNIST client; (b) visualized the SVHN client; (c) visualized the USPS client; (d) visualized the SynthDigits client; (e) visualized the MNIST-M client.

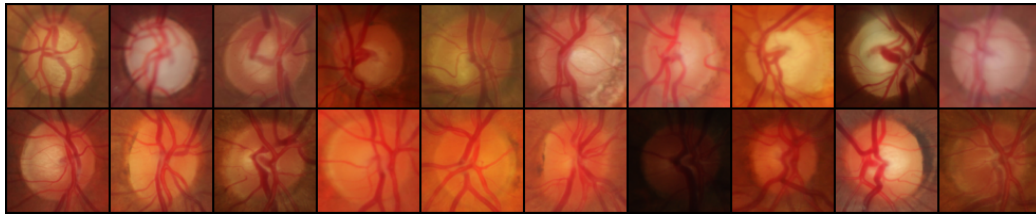
B.1.2. RETINA DATASET



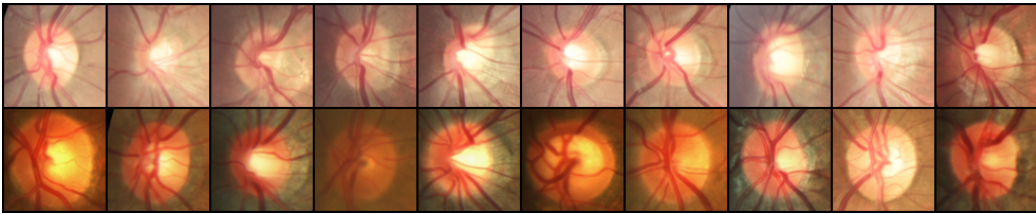
(a)



(b)



(c)

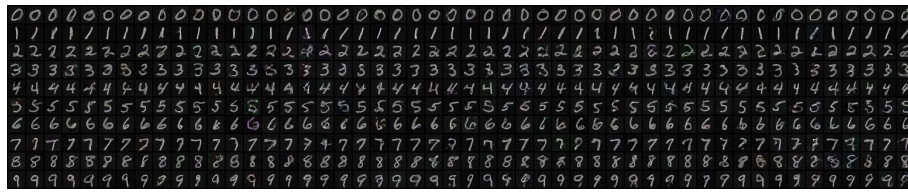


(d)

Figure 5. Visualization of the original retina dataset. (a) visualized the Drishti client; (b) visualized the Acrima client; (c) visualized the Rim client; (d) visualized the Refuge client

B.2. Visualization of our distilled global and local images

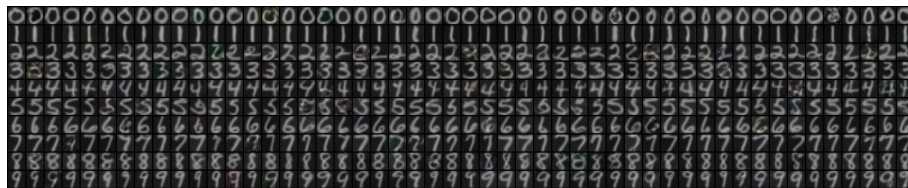
B.2.1. DIGITS DATASET



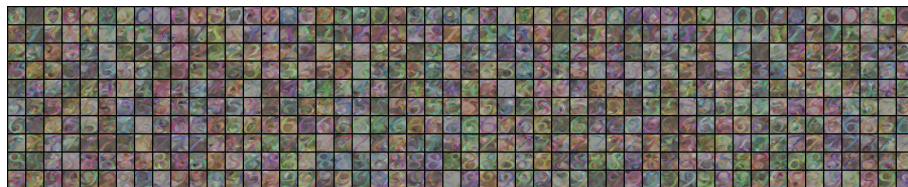
(a)



(b)



(c)



(d)



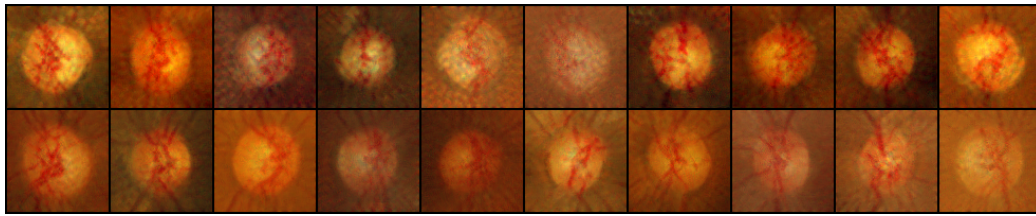
(e)



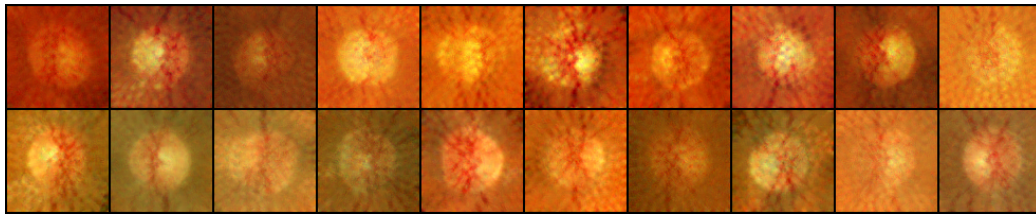
(f)

Figure 6. Visualization of the global and local distilled images from the digits dataset. (a) visualized the MNIST client; (b) visualized the SVHN client; (c) visualized the USPS client; (d) visualized the SynthDigits client; (e) visualized the MNIST-M client; (f) visualized the server distilled data.

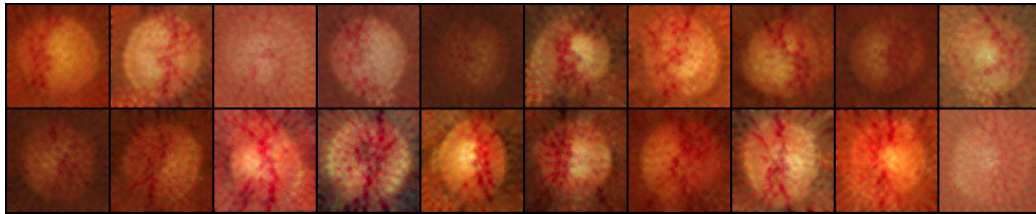
B.2.2. RETINA DATASET



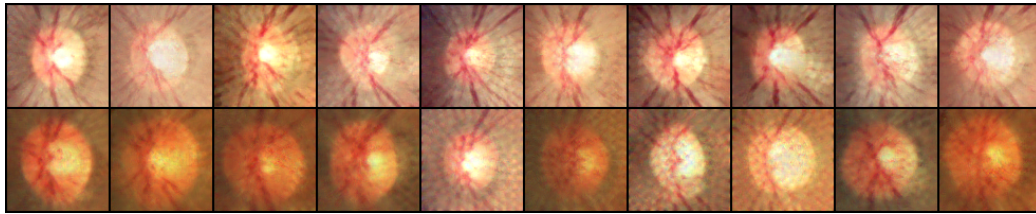
(a)



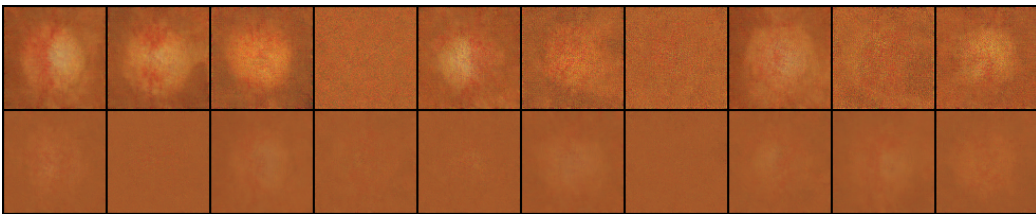
(b)



(c)



(d)



(e)

Figure 7. Visualization of the global and local distilled images from retina dataset. (a) visualized the Drishti client; (b) visualized the Acrima client; (c) visualized the Rim client; (d) visualized the Refuge client; (e) visualized the server distilled data.

B.3. Visualization of the heterogeneity of the datasets

B.3.1. DIGITS DATASET

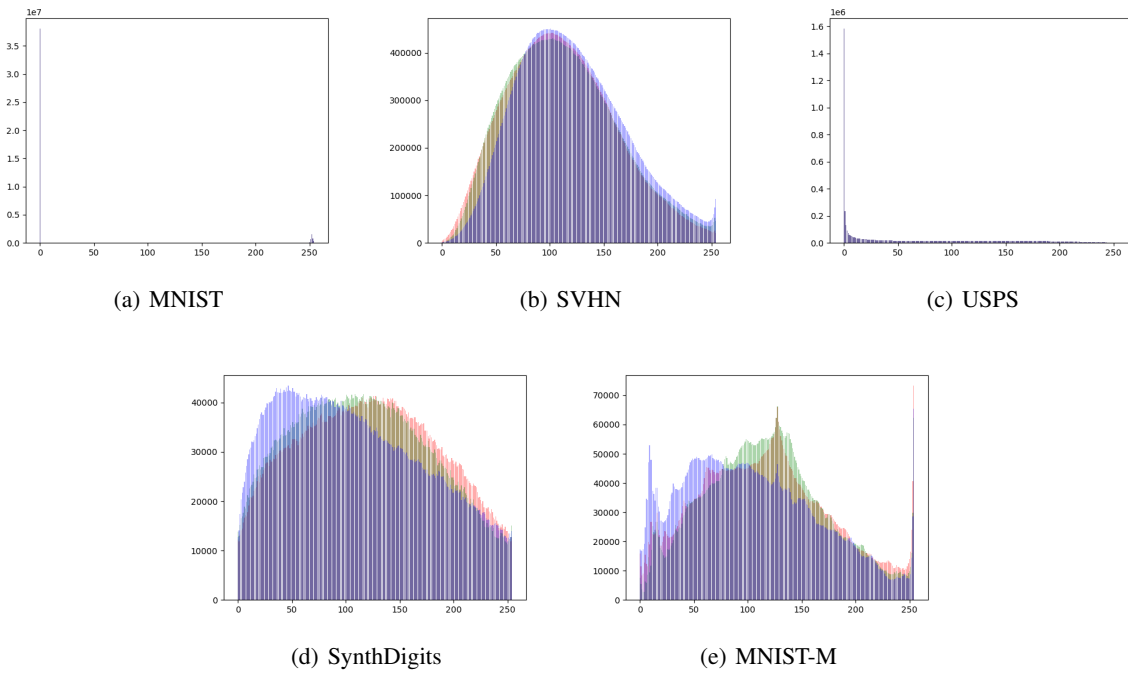
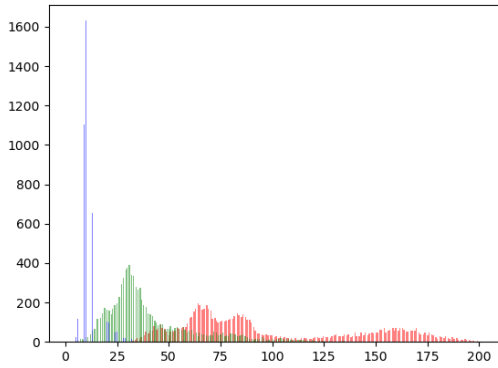
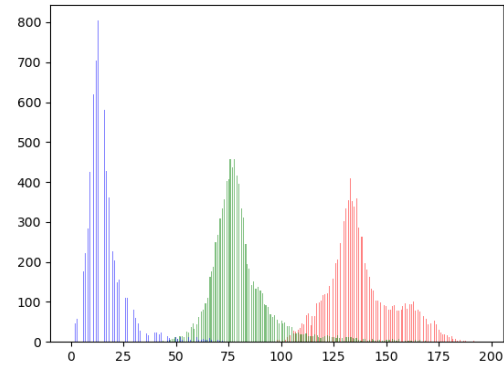


Figure 8. Histogram for the frequency of each RGB value in original *Digits*. The red bar represents the count for R; the green bar represents the frequency of each pixel for G; the blue bar represents the frequency of each pixel for B. One can observe the distributions are very different. Note that figure (a) and figure (c) are both greyscale images with most pixels lying in 0 and 255.

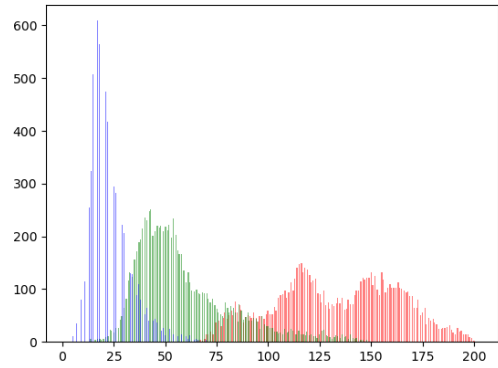
B.3.2. RETINA DATASET



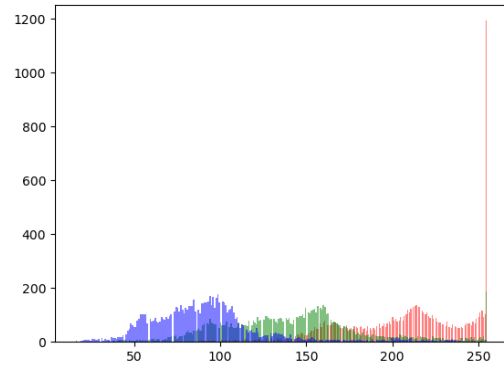
(a) Drishti



(b) Acrima



(c) RIM



(d) REFUGE

Figure 9. Histogram for the frequency of each RGB value in original *Retina*. The red bar represents the count for R; the green bar represents the frequency of each pixel for G; the blue bar represents the frequency of each pixel for B.

B.4. Model architecture

For our benchmark experiments, we use ConvNet to both distill the images and train the classification network.

Table 7. ResNet 18 architecture. For convolutional layer (Conv2D), we list parameters with sequence of input and output dimension, kernel size, stride and padding. For max pooling layer (MaxPool2D), we list kernel and stride. For fully connected layer (FC), we list input and output dimension. For BatchNormalization layer (BN), we list the channel dimension.

Layer	Details
1	Conv2D(3, 64, 7, 2, 3), BN(64), ReLU
2	Conv2D(64, 64, 3, 1, 1), BN(64), ReLU
3	Conv2D(64, 64, 3, 1, 1), BN(64)
4	Conv2D(64, 64, 3, 1, 1), BN(64), ReLU
5	Conv2D(64, 64, 3, 1, 1), BN(64)
6	Conv2D(64, 128, 3, 2, 1), BN(128), ReLU
7	Conv2D(128, 128, 3, 1, 1), BN(64)
8	Conv2D(64, 128, 1, 2, 0), BN(128)
9	Conv2D(128, 128, 3, 1, 1), BN(128), ReLU
10	Conv2D(128, 128, 3, 1, 1), BN(64)
11	Conv2D(128, 256, 3, 2, 1), BN(128), ReLU
12	Conv2D(256, 256, 3, 1, 1), BN(64)
13	Conv2D(128, 256, 1, 2, 0), BN(128)
14	Conv2D(256, 256, 3, 1, 1), BN(128), ReLU
15	Conv2D(256, 256, 3, 1, 1), BN(64)
16	Conv2D(256, 512, 3, 2, 1), BN(512), ReLU
17	Conv2D(512, 512, 3, 1, 1), BN(512)
18	Conv2D(256, 512, 1, 2, 0), BN(512)
19	Conv2D(512, 512, 3, 1, 1), BN(512), ReLU
20	Conv2D(512, 512, 3, 1, 1), BN(512)
21	AvgPool2D
22	FC(512, num_class)

Table 8. ConvNet architecture. For convolutional layer (Conv2D), we list parameters with sequence of input and output dimension, kernel size, stride and padding. For max pooling layer (MaxPool2D), we list kernel and stride. For fully connected layer (FC), we list input and output dimension. For GroupNormalization layer (GN), we list the channel dimension.

Layer	Details
1	Conv2D(3, 128, 3, 1, 1), GN(128), ReLU, AvgPool2d(2,2,0)
2	Conv2D(128, 118, 3, 1, 1), GN(128), ReLU, AvgPool2d(2,2,0)
3	Conv2D(128, 128, 3, 1, 1), GN(128), ReLU, AvgPool2d(2,2,0)
4	FC(1152, num_class)

B.5. Training details

We provide detailed settings for experiments conducted in Table 9 for digits and Table 10 for the retina.

Table 9. Digits settings for all federated learning, including the number of training and testing examples, and local update epochs. Image per class is the number of distilled images used for distribution matching only in FEDLGD.

DataSets	MNIST	SVHN	USPS	SynthDigits	MNIST-M
Number of clients	1	1	1	1	1
Number of Training Samples	60000	73257	7291	10000	10331
Number of Testing Samples	10000	26032	2007	2000	209
Number of Global Held-out Samples	209	209	209	209	209
Image per Class	10,50	10,50	10,50	10,50	10,50
Local Update Epochs	1,2,5	1,2,5	1,2,5	1,2,5	1,2,5
Local Distillation Update Epochs	100, 200, 500	100, 200, 500	100, 200, 500	100, 200, 500	100, 200, 500
global Distillation Update Epochs	500, 1000, 2000	500, 1000, 2000	500, 1000, 2000	500, 1000, 2000	500, 1000, 2000
λ	10	10	10	10	10

Table 10. Retina settings for all federated learning, including the number of training and testing examples and local update epochs. Image per class is the number of distilled images used for distribution matching only in FEDLGD.

DataSets	Drishti	Acrima	RIM	Refuge
Number of clients	1	1	1	1
Number of Training Samples	82	605	385	1000
Number of Testing Samples	19	100	100	200
Number of Global Held-out Samples	19	19	19	19
Image per class	10	10	10	10
Local Update Epochs	1,2,5	1,2,5	1,2,5	1,2,5
Local Distillation Update Epochs	100, 200, 500	100, 200, 500	100, 200, 500	100, 200, 500
global Distillation Update Epochs	500, 1000, 2000	500, 1000, 2000	500, 1000, 2000	500, 1000, 2000
λ	0.1	0.1	0.1	0.1

B.6. Convergence curves

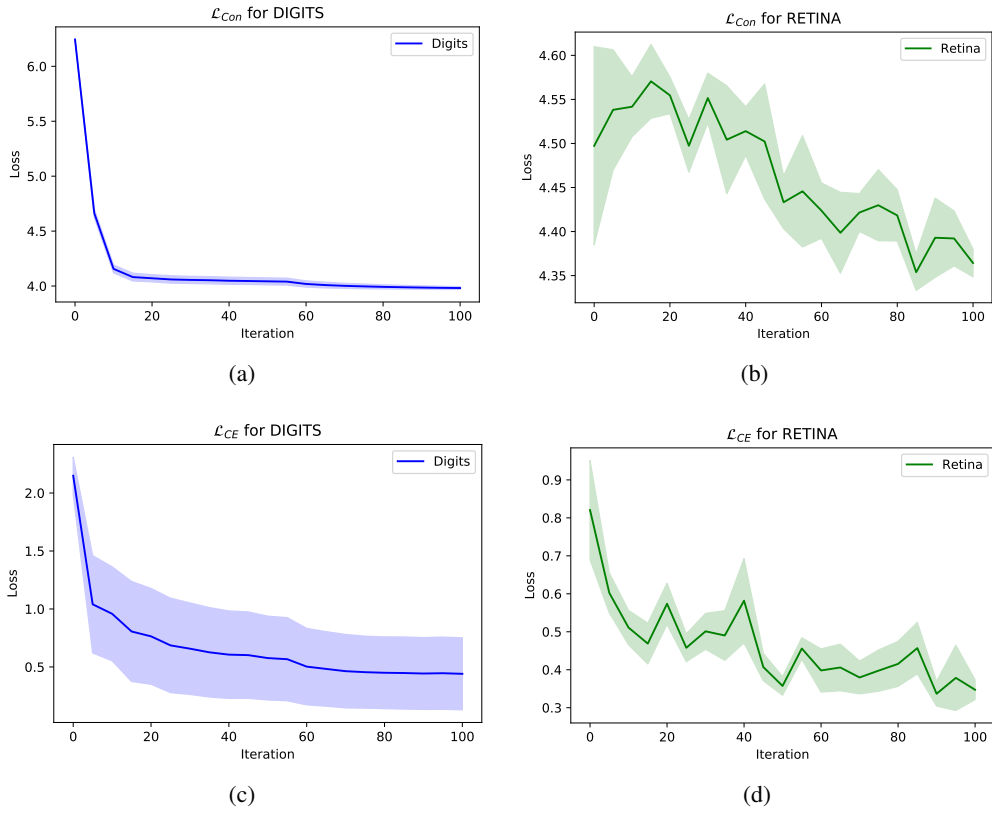


Figure 10. Averaged regularization loss for DIGITS and RETINA experiments. The decreasing regularization losses \mathcal{L}_{Con} indicate the local model is rectified by global virtual data and can learn homogeneous local features.

B.7. Visualization on Global Virtual Data in Stage 2 of FEDLGD

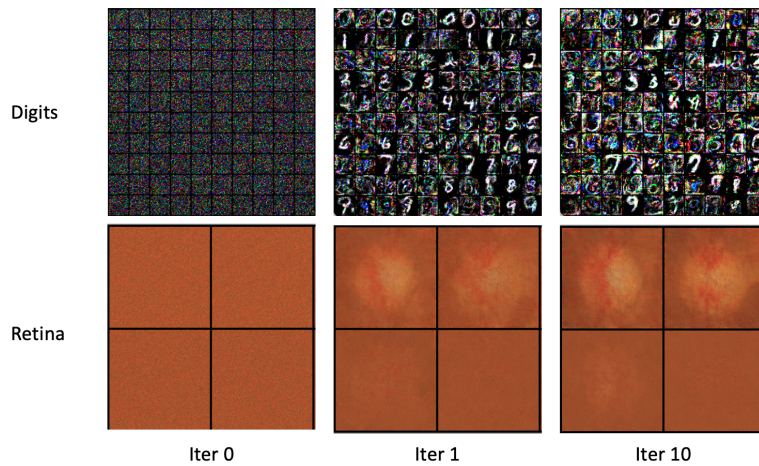


Figure 11. The updates of global synthetic data for DIGITS and RETINA. During our local-global distillation, we will update our global virtual data until $t=7$. During the process, we will update the virtual data for 10 iterations. We show the virtual data in iteration 0, 1, and 10.

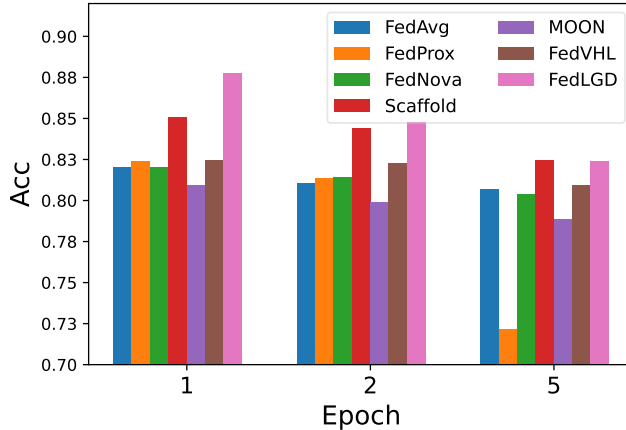


Figure 12. Comparison on model performances under different local epochs.

Table 11. FEDLGD we show the test accuracy if we use global virtual data to perform local training and test on the testing sets. One can observe that as batch size decreases, the test performance increases. In our experiments, we use batch size = 32.

Digits	MNIST	SVHN	USPS	SynthDigits	MNIST-M	Avarage
8	73.6	47.2	74.4	46.7	51.2	58.6
16	68.0	52.4	73.5	43.7	47.9	57.1
32	82.4	57.8	85.5	52.9	61.7	68.0
64	91.2	63.8	88.0	56.4	68.9	72.7

One important benefit of FEDLGD is we obtain global virtual data after FL training (Figure 11). The data are useful for rectifying local training, and furthermore, we consider a potential incentive mechanism that can reward clients who join the federation. On the other hand, although the intuitive purpose of the data is to regularize local training, we found that it actually contains information that is beneficial for local classification tasks. Therefore, we train the classification model on global virtual data and test on clients’ local test data. In addition, we vary the batch size to evaluate how it correlates with our global virtual data training and show the results in Table 11 Surprisingly, training with global virtual data only can achieve comparable results, and we consider it a very promising outcome as our global virtual data does capture useful utility.

B.8. Analysis of Local Epoch

Aggregating at different frequencies is known as an important factor that affects FL behavior. Here, we vary the local epoch $\in \{1, 2, 5\}$ to train all models. Figure 12 shows the result of test accuracy under different epochs. One can observe that as the local epoch increases, the performance of FEDLGD would drop. This is because doing gradient matching requires the model to be trained to an intermediate level, and if local epochs increase, the loss of DIGITS models will drop significantly. As a result, FEDLGD cannot generate good quality global virtual data, which degrades performance. As our future work, we will investigate the tuning of the learning rate in the early training stage to alleviate the effect.

B.9. Membership Inference Attack

It has been shown that a trained model is prone to suffer from several privacy attacks such as Membership Inference Attack (MIA) (Shokri et al., 2017). In MIA, the attackers have a list of query data, and the purpose is to determine whether the query data belongs to the original training set. As discussed in (Dong et al., 2022; Xiong et al., 2022), using distilled data to train a target model can defend against multiple attacks up to a certain level. We will especially apply MIA to test whether our work can defend against privacy attacks. In detail, we perform MIA directly on models trained with FedAvg (using the original data set) and FEDLGD (using the synthetic dataset). Furthermore, we test on the model trained with our distilled global synthetic data. We show the attack results in Figure 13 following the evaluation in (Carlini et al., 2022a). If the ROC curve is the same as the diagonal dash line, it means that the membership cannot be inferred. One can observe that models

trained with synthetic data have a ROC curve that is closer to the diagonal line, indicating that the membership is harder to be attacked.

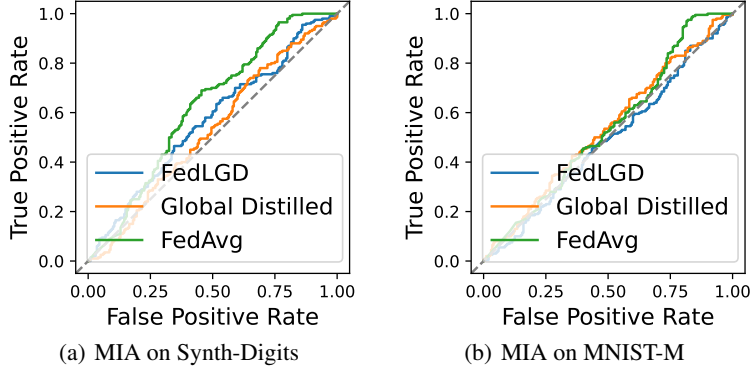


Figure 13. MIA attack results on models trained with FedAvg (using original dataset), FedLGD (using distilled virtual dataset), and distilled global virtual data. If the ROC curve is the same as diagonal line, it means the membership cannot be inferred. One can observe the ROC curve for models trained with synthetic data is closer to the diagonal line, which indicates the membership information is harder to be inferred.

C. Related work of Heterogeneous Federated Learning

FL trains the central model over a variety of distributed clients that contain non-iid data. We detailed each of the SOTA methods we compared in Section 4 below.

FedAvg (McMahan et al., 2017) The most popular aggregation strategy in modern FL, Federated Averaging (FedAvg) (McMahan et al., 2017), averages the uploaded clients’ model as the updated server model. Mathematically, the aggregation is represented as $w^{t+1} = w^t - \eta \sum_{i \in S_t} \frac{|D_i|}{n} \Delta w_k^t$ (Li et al., 2021a). Because FedAvg is only capable of handling Non-IID data to a limited degree, current FL studies proposed improvements in either local training or global aggregation based on it.

FedProx (Li et al., 2020a) FedProx improves local training by directly adding a L_2 regularization term, $\mu, \frac{\mu}{2} \|w - w^t\|^2$ controlled by hyperparameter μ , in the local objection function to shorten the distance between the server and the client distance. Namely, this regularization enforces the updated model to be as close to the global optima as possible during aggregation. In our experiment, we carefully tuned μ to achieve the current results.

FedNova (Wang et al., 2020) FedNova aims to tackle imbalances in the aggregation stage caused by different levels of training (e.g., a gap in local steps between different clients) before updating from different clients. The idea is to make larger local updates for clients with deep level of local training (e.g., a large local epoch). This way, FedNova scales and normalizes the clients’ model before sending them to the global model. Specifically, it improves its objective from FedAvg to $w^{t+1} = w^t - \eta \frac{\sum_{i \in S_t} |D^i| \tau_i}{n} \sum_{i \in S_t} \frac{|D^i| \Delta w_k^t}{n \tau_i}$ (Li et al., 2021a).

Scaffold (Karimireddy et al., 2020) Scaffold introduces variance reduction techniques to correct the ‘clients drift’ caused by gradient dissimilarity. Specifically, the variance on the server side is represented as v , and on the clients’ side is represented as v_i . The local control variant is then added as $v_i - v + \frac{1}{\tau_i \eta} (w^t - w_i^t)$. At the same time, the Scaffold adds the drift on the client side as $w^t = w^t - \eta (\Delta(w_i; b) - v_i^t + v)$ (Li et al., 2021a).

Virtual Homogeneous Learning (VHL) (Tang et al., 2022) VHL proposes to calibrate local feature learning by adding a regularization term with global anchor for local training objectives $\mathbb{E}_{(x,y) \sim P_k} l(\rho \circ \psi(x), y) + \mathbb{E}_{(x,y) \sim P_v} l(\rho \circ \psi(x), y) + \lambda \mathbb{E}_y d(P_k(\psi(x)|y), P_c(\psi(x)|y))$. They theoretically and empirically show that adding the term can improve the FL performance. In the implementation, they use untrained StyleGAN (Karras et al., 2019) to generate global anchor data and leave it unchanged during training.

A comprehensive experimental study of FL can be found here ([Li et al., 2021a](#)). Also, a survey of heterogeneous FL is here ([Zhu et al., 2021](#)).